Impact of full-azimuth and long-offset acquisition on Full Waveform Inversion in deep water Gulf of Mexico

Sabaresan Mothi*, Katherine Schwarz, Huifeng Zhu, CGG

Abstract

FWI currently relies primarily on transmitted energy, which in deep water settings requires very long offsets. If the water bottom depth is greater than 1 km, near to middle offsets (offsets less than 6 km) have reflections as the early arrivals, but these are more difficult to use for FWI because they contain density information. For most deep water wide azimuth towed streamer (WATS) surveys with a maximum offset of around 8.5 km, only the offsets greater than 6 km contain refractions and diving wave energy that are useful for FWI. Additionally, in conventional WATS acquisitions, the penetration depth of the transmitted energy is restricted by the limited surface offsets, thereby producing velocity updates that are more prone to acquisition-related artifacts. In this case study, we evaluate the benefits of full-azimuth and long offset acquisition for determining the velocities of complex overburden in a deep water region of the Gulf of Mexico.

Introduction

Because of the recent advances in imaging technology, we now look in the direction of improving the resolution of the underlying velocity model to enhance the subsurface image. Until recently, almost all approaches were based on picking events from migrated offset/angle gathers and reducing gather curvature by ray tracing. Alternatively, wave-equation-based full waveform inversion (FWI) is based on minimizing mismatch in the data space and can theoretically achieve a resolution of half the seismic data's recorded wavelength (Tarantola, 1984; Pratt et al., 1998; Sirgue et al., 2004; Virieux et al., 2009). Several successful applications of FWI have resulted in high quality velocity models in various settings, such as ocean bottom cable (Sirgue et al., 2009; Ratcliffe et al., 2011), towed streamer data in deep water (Bi et al., 2012), and land data (Mothi et al., 2012).

Most applications of FWI rely on transmitted energy for determining velocities. The major shortcoming of this method is that the extent of velocity update is limited by the offset range in the acquired data. Using towed-streamer acquisition, the penetration depths of transmitted energy are limited to a couple of kilometers below the water bottom in deep water regions of the Gulf of Mexico (GOM). To overcome this, FWI may be used with seismic reflections as proposed in Tarantola's pioneer work (1984), but this requires knowledge of the densities. Migration-based waveform inversion that uses reflected energy appears promising (Symes et al., 1991; Chavent et al., 1994; Clément et al., 2001; Xu et al., 2012). However, these methods have not yet been widely adopted for real data.

In this paper, we use transmitted energies to update the velocities in Keathley Canyon, GOM using long offsets (up to 18 km) and full-azimuth (up to 10 km) streamer data with variable depth tow. The benefits of low-frequency content in the broadband acquisition scheme for FWI were demonstrated in a North Sea example (Jupp et al., 2012). Here, we use a staged methodology to utilize the wide range of offsets and also investigate the impact of long offsets and full azimuth data on velocity inversion.

Study Area

The study area is in the deep water GOM, in an area characterized by sedimentary basins with faults, carapaces, and complex salt structures. The staggered configuration of two streamer boats (F. Mandroux, personal communication, 2012) allows ultra-long offsets of over 18 km in the inline direction (Figure 1a). The study uses east-west and north-south sail lines (Figure 1b), yielding full azimuth coverage assuming source-receiver reciprocity (Figure 1c). Acquisition with variable-depth towed streamers results in diversity of the receiver ghost notch (Soubaras et al., 2010), creating significant low-frequency content at far offsets that can aid initial FWI iterations.

FWI Components

The acquired shot gathers are minimally processed with a mild denoise flow to remove low frequency swell noise and spikes. The shot records are muted to prevent any reflection energy and surface-related reflection multiples from interfering with the velocity updates. The far field source signature is deghosted for the source ghost to obtain the source wavelet for the inversion. We use a TTI acoustic model and the FWI only updates the velocity along the tilt axis V_0 using transmitted energy (Zhang et al, 2011). The anisotropic parameters δ and ε are derived using well logs and 1D inversion, and the tilt axis is assumed to be perpendicular to the plane of the bedding. The starting velocity model is obtained using two iterations of ray-based tomography with beam migration to obtain a good starting velocity trend and prevent FWI from converging to a local minimum.

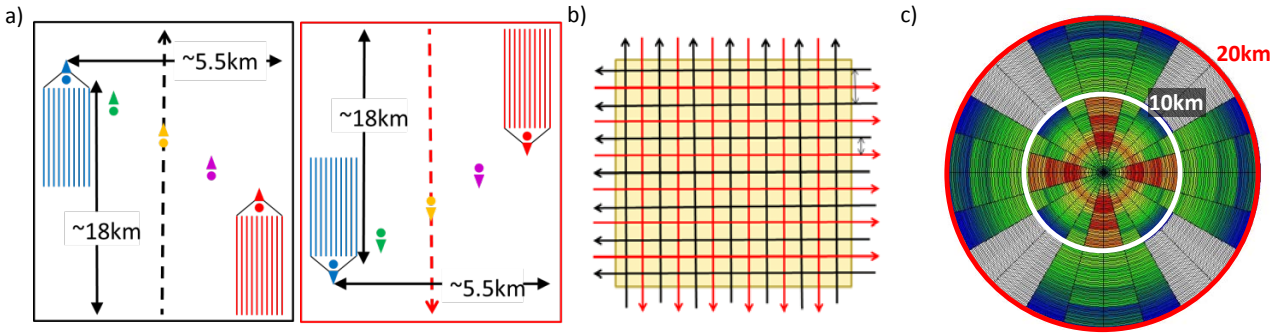

Figure 1: a) Staggered acquisition configuration; b) Sail lines; c) Rose diagram with reciprocity. The white line denotes 10 km offset, and the red line denotes 20 km offset.

Offset Stripping Inversion Approach

We start with the lowest usable frequency content in the data, i.e. from 2-3 Hz. The data is split into 3 offset classes: conventional offsets (less than 8 km), long offsets (8–12 km), and ultra-long offsets (greater than 12 km). Structural horizons determined by the maximum penetration depth of diving waves for the starting model and available offset ranges are used to constrain the regions of velocity updates. We start with the shallow velocity updates using several iterations of FWI on the conventional-offset data at 3 Hz. Following this, the long offsets are included in the inversion, and the updates now cover the shallow and deeper sections. This process is repeated for the ultra-long offsets. At this stage, we have 3 Hz inversion for the shallow overburden using all the offsets and 3 Hz data. Now we switch to the multi-scale approach and invert up to 7 Hz, with increments of 1 Hz, using all the offsets.

Impact of Long Offsets

Using this approach, we perform two inversion tests. The first imitates a traditional wide azimuth acquisition (WAZ) receiver spread with maximum inline and crossline offsets of 7.5 km and 4 km respectively. The second test uses no offset restrictions. Test #1 produces velocity updates in deeper sections that are highly oscillatory in nature (yellow outline in Figure 2a), and the carbonate section is incorrectly inverted as a slow velocity section (green outline in Figure 2a); we attribute this to insufficient diving ray penetration. From test #2 (Figure 2b), we see that updates are more characteristic of the geology and do not have the same artificial oscillation. Furthermore, offset gathers from beam migrations (Figure 2) also suggest that the perturbation from test #1 results in over-corrected gathers in the area immediately above the carbonate section. Test #2 produces flatter gathers.

Impact of Full Azimuth

The orthogonal acquisition provides data with a variety of azimuth information. With increased crossline offset, we expect better illumination and transmission energy penetration from the transverse direction as well. In order to understand the benefits of this acquisition configuration, the above inversion scheme is applied to only conventional-offset data using 1) only north-south shotlines and 2) both north-south and east-west shotlines (full azimuth). From the 3 Hz FWI results (after 1 iteration) in Figure 3, we observe that the inversion suffers from a north-south striping pattern, i.e. an acquisition footprint, when using limited azimuth information. The sparse sampling of the acquisition in the crossline direction compared to the inline direction may cause these artifacts. This effect tends to be cumulative. In contrast, inversion using the full azimuth data does not suffer from these issues.

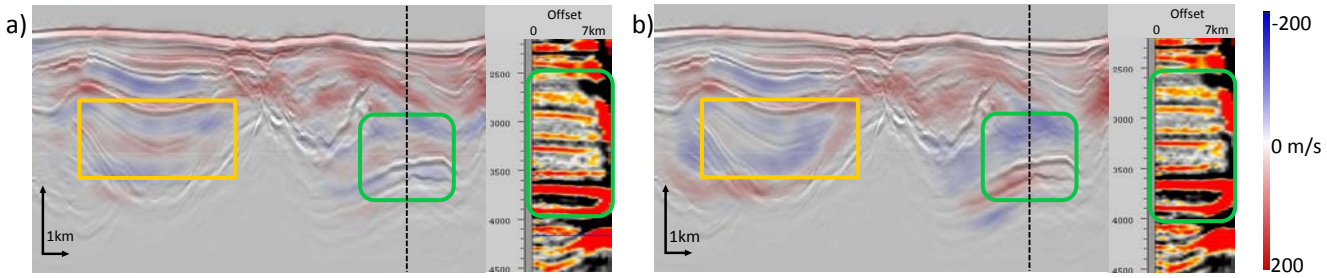

Figure 2: Perturbation and beam migration offset gathers (gather location indicated by the black dotted line) using a) WAZ offset ranges; b) full azimuth (FAZ), long offsets.

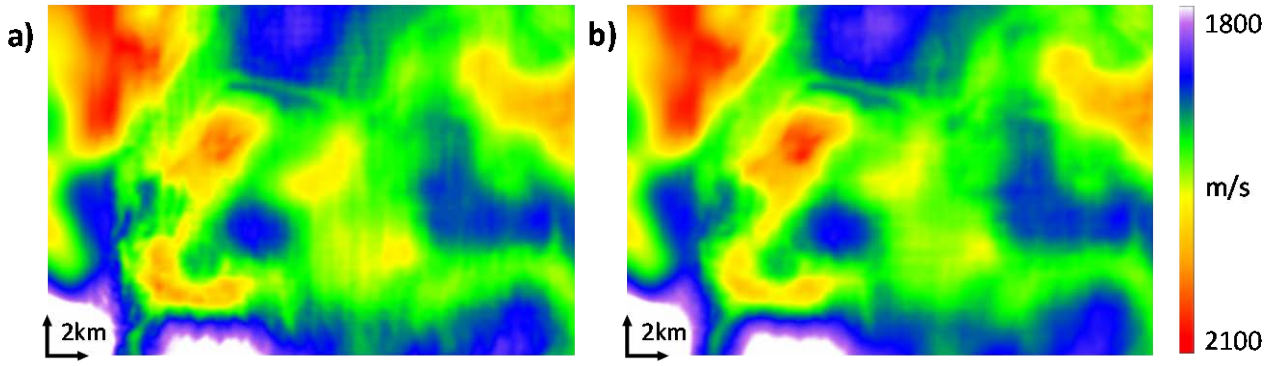

Figure 3. Depth slice @ 2250 m: V_0 after FWI using a) north-south shots only; b) north-south & east-west shots

Inversion Results

With the offset stripping and multi-scale approach, we perform the inversion using full-azimuth and long-offset data for frequencies up to 7 Hz. The velocity model in Figures 4b and d clearly shows that the inversion produces geological models and tracks the faults and high velocity condensed sections directly above the top of salt. The carbonates and the shale bodies are detected by the inversion. The PSDM stack response is also improved in Figure 4d after the inversion. Furthermore, beam migrations (Figure 5) show that the gather flatness is mostly improved, and the detailed velocities result in more consistent curvature across the orthogonal azimuths. The improvement from the gathers is subtle because the starting velocity model had two iterations of reflection tomography.

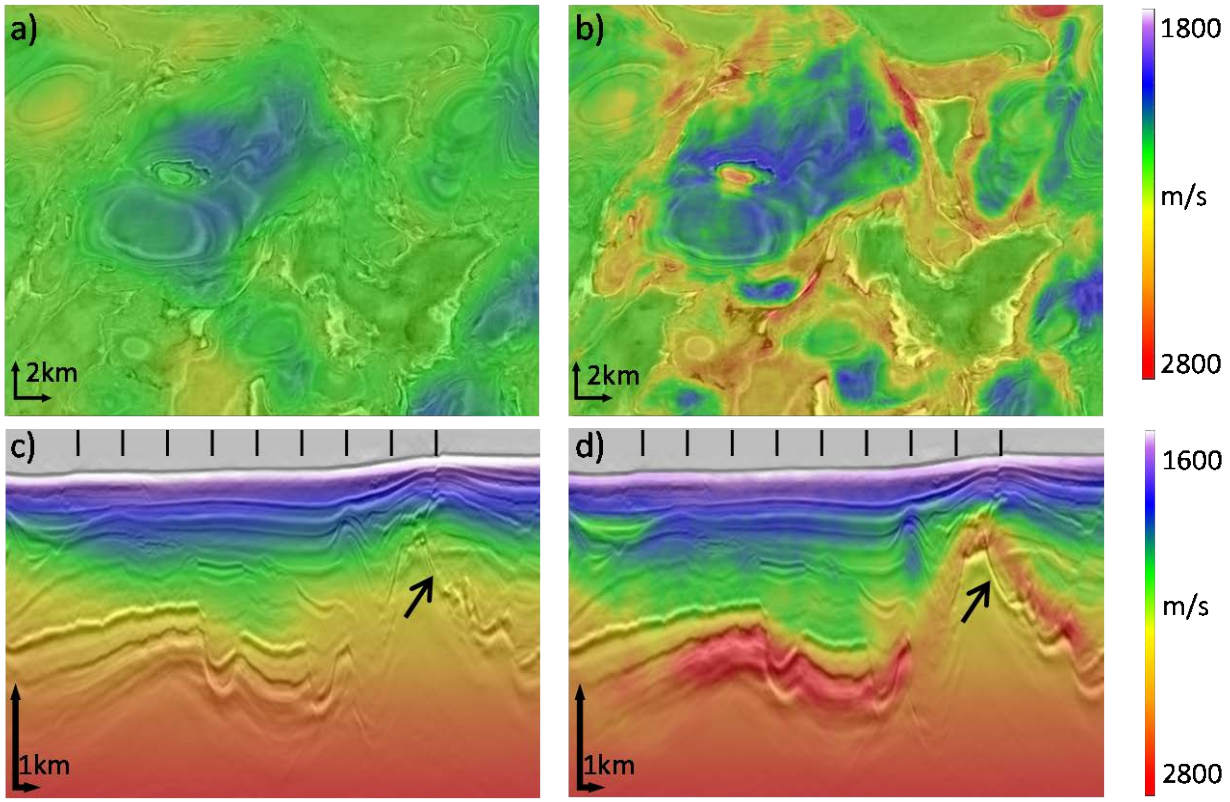

Figure 4: Depth slice @ 2820 m of V_0 with the corresponding PSDM: a) before FWI; b) after FWI
Inline view of V_0 with the corresponding PSDM: c) before FWI; d) after FWI
Black vertical lines in c) and d) indicate the location of the gathers in Figure 5. Black arrows in c) and d) indicate top of salt.

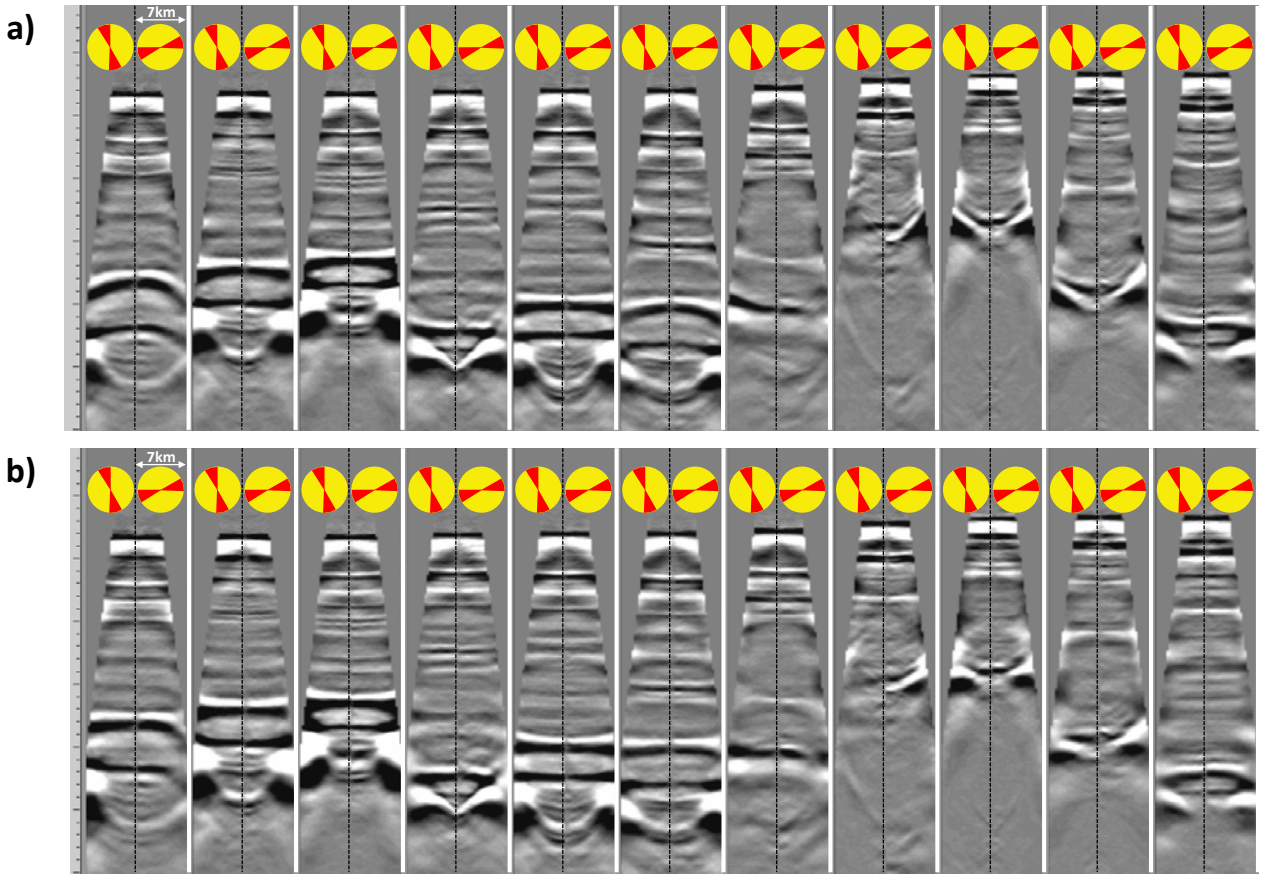

Figure 5. Beam migration offset gathers from orthogonal azimuths (with source-receiver azimuth indicated above the gather) at 11 locations using velocity a) before FWI; b) after FWI.

Discussion and Conclusion

Our results clearly show the image improvement that additional offsets and azimuths bring to the inversion in terms of illuminating more subsurface angles and deeper sections. The approach we demonstrate produces interpretive models that characterize the different geological sections.

References

Bi, H., and S. Mothi, 2012, Application of FWI to resolve gas cloud velocity anomaly in deep water Gulf of Mexico: 74th Conference and Exhibition, EAGE, Extended Abstracts, W014.

Clément, F., G. Chavent, and S. Gómez, 2001, Migration-based traveltime waveform inversion of 2-D simple structures: A synthetic example: Geophysics, 66, 845–860.

Chavent, G., F. Clément, and S. Gómez, 1994, Automatic determination of velocities via migration-based traveltime waveform inversion: A synthetic data example: 64th Annual International Meeting, SEG, Expanded Abstracts, 1179–1182.

Jupp, R., A. Ratcliffe, and R. Wombell, 2012, Application of Full Waveform Inversion to variable-depth streamer data. 82nd International Annual Meeting, SEG, Expanded Abstracts, doi: 10.1190/segam2012-0613.1

Mothi, S., H. Bi, and A. Yang, 2012, Benefits of FWI in prestack depth imaging of onshore data: a Gulf Coast example: 82nd International Annual Meeting, SEG, Expanded Abstracts, doi: 10.1190/segam2012-1486.1

Pratt, R., C. Shin, and G. Hicks, 1998, Gauss-Newton and full Newton methods in frequency-space seismic waveform inversion: Geophysical Journal International, 13, 341–362.

Ratcliffe, A., C. Win, V. Vinje, G. Conroy, M Warner, A. Umpleby, I Stekl, T. Nangoo and A. Bertrand, 2011, Full waveform inversion: A North Sea OBC case study: 81st Annual International Meeting, SEG, Expanded Abstracts, 2384–2388.

Sirgue, L., O. I. Barkved, J. P. Van Gestel, O. J. Askim, and J. H. Kommedal, 2009, 3D Waveform inversion on Valhall wide-azimuth OBC: 71st Conference and Exhibition, EAGE, Extended Abstracts, U038.

Sirgue, L., and R. G. Pratt, 2004, Efficient waveform inversion and imaging: A strategy for selecting temporal frequencies: Geophysics, 69, 231–248.

Soubaras, R., and R. Dowle, 2010, Variable-depth streamer – a broadband marine solution: First Break, Vol. 28 No. 12, 89–96.

Symes, W. W., and J. J. Carazzone, 1991, Velocity inversion by differential semblance optimization: Geophysics, 56, 654–663.

Tarantola, A., 1984, Inversion of seismic reflection data in the acoustic approximation: Geophysics, 49, 1259–1266.

Virieux, J., and S. Operto, 2009, An overview of full-waveform inversion in exploration geophysics: Geophysics, 74, no. 6, WCC1–WCC26.

Xu, S., D. Wang, F. Chen, G. Lambaré, and Y. Zhang, 2012, Full waveform inversion for reflected seismic data: 74th Conference and Exhibition, EAGE, Extended Abstracts, W024.

Acknowledgments

We thank CGG for permission to publish these results. We also acknowledge Yu Zhang, Andrew Ratcliffe, and Graham Conroy for their support with the inversion engine. We appreciate the input from Tony Huang, Kyle Huang, Qiaofeng Wu, and Yunfeng Li.